Crystal Structure and Spectroscopic and Redox Properties of the Iron–Sulphur Cluster Compound $[NEt_4]_2[Fe_4S_4(SC_6H_4NH_2\text{-}4)_4]$†

Timothy J. Ollerenshaw and C. David Garner *
Department of Chemistry, The University, Manchester M13 9PL
Barbara Odell
Shell Research, Sittingbourne, Kent M39 8AG
William Clegg *
Department of Inorganic Chemistry, The University, Newcastle upon Tyne NE1 7RU

A 4Fe-ferrodoxin analogue involving functional thiolato-groups, $[Fe_4S_4(SC_6H_4NH_2\text{-}4)_4]^{2-}$, has been prepared and, as its $[NEt_4]^+$ salt, characterised by *X*-ray crystallography, u.v.–visible, ^1H and ^{13}C n.m.r. spectroscopy, and electrochemistry. The geometry of the Fe_4S_4 core is very similar to that previously established for other clusters of this type and possesses crystallographic S_4 symmetry; the Fe_4 tetrahedron is slightly compressed along the S_4 axis and the Fe ··· Fe edges group as four shorter [2.741(1) Å] and two longer [2.767(1) Å] distances. The NH_2 groups do not participate in any secondary bonding interactions. The complex undergoes two quasi-reversible, one-electron reductions at −1.12 and −1.74 V (*vs.* saturated calomel electrode).

The chemistry of the cubane-like clusters $[Fe_4S_4(SR)_4]^{2-}$ has been extensively developed and the role of these clusters as structural and electronic analogues of 4Fe-ferredoxin protein sites has been amply demonstrated.[1–3] A large number of such clusters has been prepared,[3] and several of them have been crystallographically characterised. Clusters for which crystal structures have been reported include arene- and alkane-thiolate clusters, such as $[Fe_4S_4(SBu^t)_4]^{2-}$ [4] and $[Fe_4S_4(SPh)_4]^{2-}$,[5] and those in which the thiolate ligands contain another functional group, such as $[Fe_4S_4(SCH_2CH_2OH)_4]^{2-}$,[6] $[Fe_4S_4(SCH_2CH_2CO_2)_4]^{6-}$,[7] and $[Fe_4S_4(SC_6H_4OH\text{-}2)_4]^{2-}$.[8] Furthermore, interest in examples of this latter type is stimulated by the possibility of the sulphur atoms of the cluster participating in hydrogen bonding, since such interactions have been detected in the crystal structures of *Peptococcus aerogenes* ferredoxin[9] and *Chromatium vinosum* High Potential Iron Protein (HiPIP),[10] with nearby polypeptide amide linkages. Also, for thiolate ligands which possess an additional functional group, there exists the possibility of intramolecular secondary bonding interactions. This has been demonstrated for $[Fe_4S_4(SC_6H_4OH\text{-}2)_4]^{2-}$,[8] which contains one five-co-ordinate iron atom, the additional weak bond being to one of the hydroxy-groups.

We report here the preparation, crystal structure, and properties of $[NEt_4]_2[Fe_4S_4(SC_6H_4NH_2\text{-}4)_4]$, a further example of a $[Fe_4S_4(SR)_4]^{2-}$ cluster with a functional thiolate group.

Experimental

All manipulations were carried out under dinitrogen or argon in Schlenk-type apparatus. Solvents were purged of dioxygen before use. Acetonitrile (Aldrich 99%) was distilled from calcium hydride under a dinitrogen atmosphere. Methanol (AnalaR grade), dimethylformamide (dmf) (B.D.H.), 4-aminothiophenol (Lancaster Synthesis), anhydrous iron(III) chloride (B.D.H. laboratory grade, unsublimed), and $[NEt_4]Cl$ (B.D.H.) were used as obtained.

Preparation of $[NEt_4]_2[Fe_4S_4(SC_6H_4NH_2\text{-}4)_4]$.—The complex was obtained by both of the well established methods for the synthesis of $[Fe_4S_4(SR)_4]^{2-}$ cubane-like clusters: (*a*) direct synthesis;[11] (*b*) thiolate exchange.[12]

(*a*) Lithium (0.28 g, 40 mmol) was dissolved in methanol (20 cm^3) and $HSC_6H_4NH_2$-4 (5.0 g, 40 mmol) was added, to give a pale yellow solution. After stirring for *ca.* 30 min, $FeCl_3$ (1.62 g, 10 mmol) in methanol (20 cm^3) (previously filtered through Celite) was added. A reaction ensued, producing a violet-black solution. Elemental sulphur was added (0.32 g, 10 mmol), and the mixture stirred for *ca.* 10 min. It was then filtered, and the filtrate treated with an excess of $[NEt_4]Cl$ (1.42 g, 7.5 mmol) to give a fine black crystalline material.

(*b*) To a solution of $[NEt_4]_2[Fe_4S_4(SBu^t)_4]$[11] (3.34 g, 3.5 mmol) in acetonitrile (100 cm^3) was added solid $HSC_6H_4NH_2$-4 (2.16 g, 17 mmol), and the colour of the solution changed from golden-brown to violet-black. The reaction mixture was maintained at *ca.* 50 °C under partial vacuum for *ca.* 30 min, to remove liberated t-butyl thiol; virtually all of the solvent was then removed *in vacuo* at the same temperature. The black powder which precipitated was collected by filtration and washed with methanol (5 cm^3).

Recrystallisation was achieved by dissolving the solid in the minimum amount of warm (*ca.* 50 °C) dmf (*ca.* 70 cm^3) and the solution was filtered. Methanol (30 cm^3) was added to the warm solution and the mixture cooled slowly to −10 °C. The product separated out as black crystals, which were washed with methanol (30 cm^3) and dried *in vacuo*.

The overall yield from both synthetic routes was *ca.* 60% (Found: C, 43.1; H, 5.7; Fe, 19.7; N, 7.8; S, 23.1. Calc. for $C_{40}H_{64}Fe_4N_6S_8$: C, 43.3; H, 5.8; Fe, 20.1; N, 7.6; S, 23.1%).

The $[NBu^n_4]^+$ salt was prepared in an analogous manner to that described in (*a*) (Found: C, 50.2; H, 7.3; Fe, 16.5; N, 6.4; S, 19.1. Calc. for $C_{56}H_{96}Fe_4N_6S_8$: C, 50.4; H, 7.3; Fe, 16.8; N, 6.3; S, 19.2%).

Instrumentation.—U.v.–visible absorption spectra were measured with a Pye Unicam SP8-500 spectrophotometer. Proton n.m.r. spectra were recorded on a Varian SC300 spectrometer, ^{13}C n.m.r. spectra on a Varian XL-300 spectrometer. Electrochemical measurements were accomplished using a Princeton Applied Research system, comprising a model 175 waveform generator, a model 173 potentiostat, a model 379 coulometer, and a model 5206 two-phase lock-in analyser.

---

† Bis(tetraethylammonium) tetrakis[(4-aminobenzenethiolato)-μ_3-sulphido-ferrate].

Supplementary data available (No. SUP 56263, 5 pp.): H-atom co-ordinates, thermal parameters, other bond lengths and angles. See Instructions for Authors, *J. Chem. Soc., Dalton Trans.*, 1985, Issue 1, pp. xvii—xix. Structure factors are available from the editorial office.

Polarography was performed with a dropping-mercury electrode at 1 drop s^{-1} and at a scan rate of 5 mV s^{-1}, the reference electrode being an Ag–AgCl electrode. For cyclic voltammetric measurements a glassy carbon electrode was used; the reference electrode was a saturated calomel electrode (s.c.e.). All solutions contained *ca.* 0.05 mol dm^{-3} $Li[ClO_4]$ or $[NEt_4][ClO_4]$ as a supporting electrolyte.

Crystal Structure Determination.—Crystal data. $C_{40}H_{64}Fe_4N_6S_8$, $M = 1\,108.9$, tetragonal, $a = 13.292(1)$, $c = 14.190(2)$ Å, $U = 2\,507.1$ Å^3 (from 2θ values of 30 centred reflections), $T = 291$ K, graphite-monochromated Mo-K_α radiation, $\lambda = 0.710\,69$ Å, space group $P\bar{4}2_1c$, $Z = 2$, $D_c = 1.469$ g cm^{-3} (requiring S_4 symmetry for the anion and C_2 symmetry for the cation), $F(000) = 1\,156$, crystal size $0.7 \times 0.7 \times 0.6$ mm, $\mu = 14.9$ cm^{-1}.

Data collection and processing. Stoe-Siemens AED diffractometer, $7 < 2\theta < 50°$; data collected with all indices positive and $k \leqslant h$, and with all negative (Friedel opposites); on-line profile fitting;[13] empirical absorption correction based on azimuthal scan measurements for sets of equivalent reflections (transmission 0.30—0.35); no significant variation in intensity for three standard reflections. 3 551 Data, 2 199 unique (merging $R = 0.021$), 1 917 with $F > 4\sigma(F)$.

Structure analysis and refinement. Patterson and difference syntheses; blocked-cascade refinement on F with $w^{-1} = \sigma^2(F) + 0.0004F^2$ optimised automatically; H atoms freely refined with isotropic U for NH_2, others constrained to give C–H 0.96 Å on aromatic ring external bisectors, H–C–H 109.5° in ethyl groups; anisotropic thermal parameters for non-H atoms. Extinction correction $F_c' = F_c/(1 + xF_c^2/\sin 2\theta)^{\frac{1}{4}}$ with $x = 1.8(2) \times 10^{-6}$; absolute assignment of x and y axes by refinement of $\eta = 1.03(4)$;[14] scattering factors from ref. 15. Final $R = 0.028$ for 141 parameters, $R' = (\Sigma w\Delta^2/\Sigma wF_o^2)^{\frac{1}{2}} = 0.037$; slope of normal probability plot = 1.17. Programs: SHELXTL,[16] diffractometer control program by W. C.

Results and Discussion

Crystal Structure.—Atomic co-ordinates are given in Table 1, selected bond lengths and angles in Table 2. The structure of the anion is shown in Figure 1. The dimensions of this anionic cluster are compared with those of other $[Fe_4S_4(SR)_4]^{2-}$ clusters in Table 3. The principal structural features of the Fe_4S_4 core in $[NEt_4]_2[Fe_4S_4(SC_6H_4NH_2\text{-}4)_4]$ are similar to those of all previously reported clusters of this type, in the following respects: (*i*) the core consists of essentially concentric, imperfect Fe_4 and S_4 tetrahedra, the latter having a larger volume than the former; (*ii*) the core Fe_2S_2 faces are non-

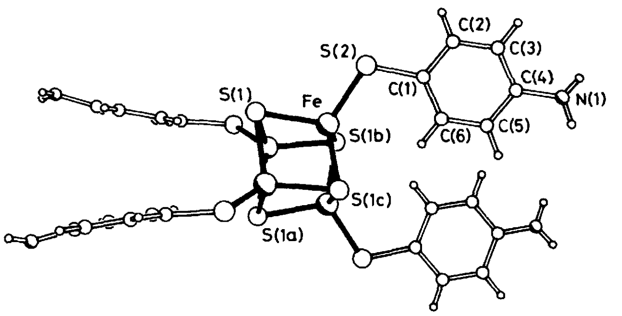

Figure 1. The structure of the anion of $[NEt_4]_2[Fe_4S_4(SC_6H_4NH_2\text{-}4)_4]$

Table 1. Atomic co-ordinates (× 10^4) for the crystallographically independent atoms of $[NEt_4]_2[Fe_4S_4(SC_6H_4NH_2\text{-}4)_4]$

Atom	*x*	*y*	*z*
Fe(1)	4 267(1)	4 261(1)	4 324(1)
S(1)	4 045(1)	4 037(1)	5 890(1)
S(2)	3 258(1)	3 201(1)	3 506(1)
C(1)	3 273(2)	3 483(2)	2 284(2)
C(2)	2 925(2)	2 760(2)	1 654(2)
C(3)	2 818(2)	2 970(2)	708(2)
C(4)	3 058(2)	3 909(2)	347(2)
C(5)	3 450(3)	4 607(3)	961(2)
C(6)	3 563(3)	4 401(3)	1 914(2)
N(1)	2 842(3)	4 162(3)	−582(2)
H(1′)	3 038(23)	4 730(26)	−771(19)
H(1″)	2 776(25)	3 717(25)	−967(22)
N(2)	5 000	0	8 859(2)
C(21)	4 437(3)	−758(3)	8 253(2)
C(22)	3 658(3)	−325(3)	7 594(3)
C(23)	4 282(2)	600(2)	9 465(2)
C(24)	3 654(3)	−5(3)	10 138(2)

Table 2. Selected bond lengths (Å) and angles (°) for the anion of $[NEt_4]_2[Fe_4S_4(SC_6H_4NH_2\text{-}4)_4]$

Fe–Fe(a)	2.767(1)	Fe–Fe(b)	2.741(1)
Fe–S(1)	2.262(1)	Fe–S(1b)	2.292(1)
Fe–S(2)	2.266(1)	S(2)–C(1)	1.773(3)
S(1)–Fe–S(1b)	104.0(1)	S(1b)–Fe–S(1c)	103.7(1)
S(1)–Fe–S(2)	110.1(1)	S(1b)–Fe–S(2)	117.6(1)
S(1c)–Fe–S(2)	115.9(1)	Fe–S(1)–Fe(b)	74.0(1)
Fe(b)–S(1)–Fe(c)	74.2(1)	Fe–S(2)–C(1)	111.3(1)

Symmetry operators: a $1 - x$, $1 - y$, z; b $1 - y$, x, $1 - z$; c y, $1 - x$, $1 - z$.

Table 3. Average dimensions of $[Fe_4S^*_4(SR)_4]^{2-}$ cubane-like clusters

R =		$C_6H_4NH_2$-4	Bu^{t}[a]	Ph[b]	CH_2Ph[c]	$CH_2CH_2CO_2$[d]	CH_2CH_2OH[e]		C_6H_4OH-2[f]
Distance/Å									
Fe–Fe	(2)[g]	2.767(1)	2.749(2)	2.730(2)	2.776(2)	2.778(3)	2.71(1)	(6)[g]	2.77(7)
	(4)	2.741(1)	2.764(3)	2.739(4)	2.732(3)	2.743(3)	2.74(1)		
Fe–S*	(4)	2.262(1)	2.274(3)	2.267(5)	2.239(4)	2.261(3)	2.24(1)	(12)	2.30(5)
	(8)	2.292(1)	2.294(2)	2.296(4)	2.310(3)	2.300(3)	2.31(1)		
Fe–S	(4)	2.266(1)	2.254(3)	2.263(3)	2.251(3)	2.250(3)	2.26(2)	(3)	2.278(7)
Fe–S*–Fe	(12)	74.1(1)	74.1(1)	73.5(1)	73.8(1)	74.1(2)	73.5(9)		74.1(1.5)
S*–Fe–S*	(12)	103.9(1)	104.0(1)	104.3(1)	104.1(1)	103.9(2)	104.3(1.4)		103.8(2.2)
S–Fe–S*[h]	(12)	110.1(1)—	107.5(1)—	100.2(1)—	100.2(1)—	109.9(2)—	109.4(3)—	(9)	106.5(1)—
		117.6(1)	117.9(1)	135.7(1)	117.3(2)	119.3(2)	119.0(3)		118.8(1)

[a] Ref. 4. [b] Ref. 5. [c] B. A. Averill, T. Herskovitz, R. H. Holm, and J. A. Ibers, *J. Am. Chem. Soc.*, 1973, **95**, 3523. [d] Ref. 7. [e] Ref. 6. [f] Ref. 8. [g] The number of distances averaged to give a particular value is given in parentheses. [h] The minimum and maximum values are given.

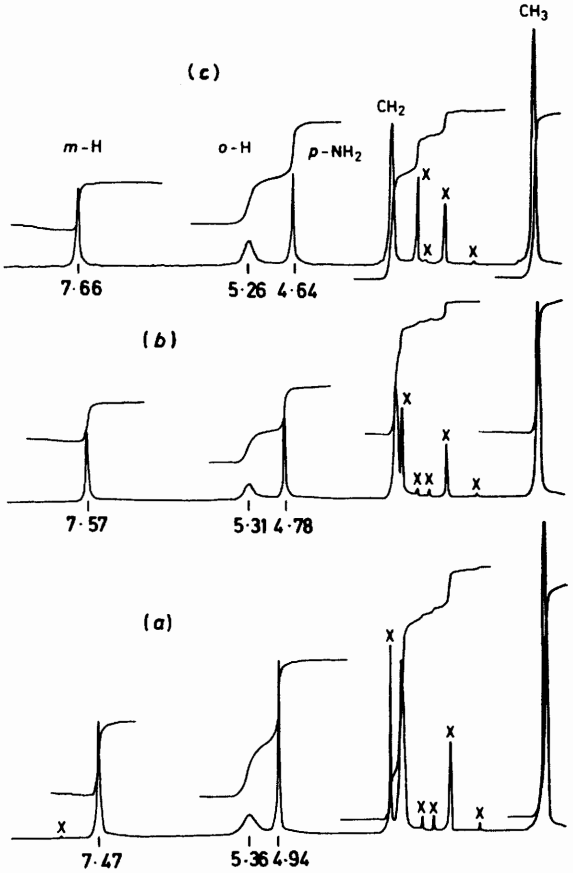

Figure 2. Proton n.m.r. spectrum of $[NEt_4]_2[Fe_4S_4(SC_6H_4NH_2\text{-}4)_4]$ in $(CD_3)_2SO$ at 25 (*a*), 75 (*b*), and 125 °C (*c*). The features marked X are due to residual solvent protons and water. Chemical shifts are in p.p.m.

planar rhombs; (*iii*) S_4 symmetry is crystallographically imposed on the cluster, but the Fe_4S_4 core has essentially D_{2d} symmetry, as is the case for $[NEt_4]_2[Fe_4S_4(SBu^t)_4]$;[4] this tetragonal distortion away from T_d symmetry is such that, with reference to the true S_4 axis of the cluster, there are four short Fe–S bonds [2.262(1) Å] approximately parallel to the axis, and eight long Fe–S bonds [2.292(1) Å] transverse to it; and (*iv*) the Fe–Fe distances occur as four shorter [2.741(1) Å] and two somewhat longer [2.767(1) Å] separations, resulting in a Fe_4 tetrahedron slightly compressed along the S_4 axis. The Fe_4S_4 core is thus subject to only small structural differences in these clusters.

No evidence of hydrogen bonding, either intermolecular or intramolecular, is found for the 4-NH_2 substituents. Intermolecular hydrogen bonding has been observed in $[NMe_4]_2[Fe_4S_4(SCH_2CH_2OH)_4]$.[6] Furthermore, the NH_2 groups do not participate in secondary bonding to Fe atoms: this would clearly be geometrically impossible within the same anion, in contrast to the co-ordination of one OH group in $[NEt_4]_2[Fe_4S_4(SC_6H_4OH\text{-}2)_4]$,[8] but also does not occur between different anions.

Electronic Spectrum.—The u.v.–visible absorption spectrum of $[NEt_4]_2[Fe_4S_4(SC_6H_4NH_2\text{-}4)_4]$ in dmf solution shows intense absorption in the region below 330 nm, with a shoulder at $\lambda_{max.}$ 499 nm ($\varepsilon_{max.}$ 16 500 dm^3 mol^{-1} cm^{-1}). Holm and co-workers[8] report a value for $\lambda_{max.}$ of 499 nm ($\varepsilon_{max.}$ 18 800 dm^3 mol^{-1} cm^{-1}) for this cluster.

Table 4. Isotropic proton shifts of $[Fe_4S_4(SC_6H_4R\text{-}4)_4]^{2-}$

	Shift/p.p.m.			
R	*ortho*	*meta*	*para*	θ_c/°C
$H^{a,b}$	+1.56	−0.89	+2.09	22
$NH_2{}^a$	+1.51	−0.60	+0.57	25
$Me^{a,b}$	+1.47	−0.86	−1.70	22
$NMe_2{}^{c,d}$	+1.48	−0.89	−0.34	30

[a] In $(CD_3)_2SO$ solution. [b] R. H. Holm, W. D. Phillips, B. A. Averill, J. J. Mayerle, and T. Herskovitz, *J. Am. Chem. Soc.*, 1974, **96**, 2109. [c] In CD_3CN solution. [d] Ref. 5.

Table 5. Values of $E_{\frac{1}{2}}$/V for the 2−/3− and 3−/4− redox processes of $[NEt_4]_2[Fe_4S_4(SC_6H_4NH_2\text{-}4)_4]^a$ in dmf solution

Method	2−/3−	3−/4−
D.c. polarography[b]	−1.11	−1.66
Differential pulse polarography[b]	−1.13	−1.69
A.c. polarography[b]	−1.14	−1.72
Cyclic voltammetry[c]	−1.12	−1.74
Differential pulse polarography[d]	−1.20	−1.86

[a] Concentration 1.5 × 10^{-3} mol dm^{-3}. [b] Measured at 22 °C, potentials *vs.* Ag–AgCl. [c] Measured at 22 °C, potentials *vs.* s.c.e., with a scan rate of 100 mV s^{-1}. [d] Ref. 8; *vs.* s.c.e.

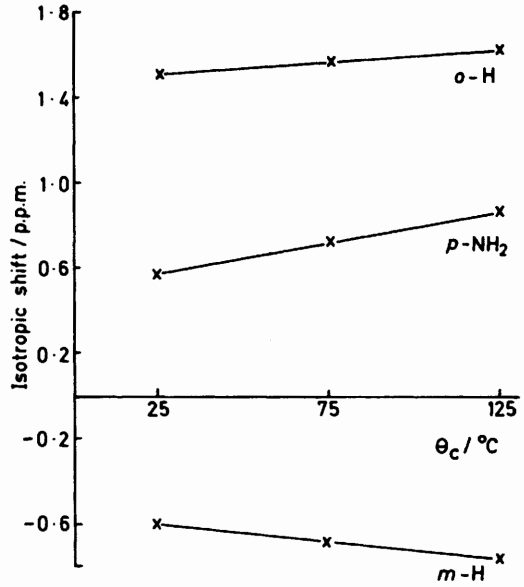

Figure 3. The temperature dependence of the isotropic shifts of the ^1H resonances of $[Fe_4S_4(SC_6H_4NH_2\text{-}4)_4]^{2-}$

Proton N.M.R. Spectra.—Proton n.m.r. spectra (300 MHz) of the compound in $(CD_3)_2SO$ solution at 25, 75, and 125 °C are shown in Figure 2. Holm and co-workers[8,*] reported the following chemical shift values obtained from a CD_3CN solution: −4.21 (NH_2), −5.66 (*o*-H), and −7.47 p.p.m. (*m*-H). Our results are in concordance with these and we draw attention to the solvent dependence of the NH_2 resonance, which, at 25°C in $(CD_3)_2SO$, is at 4.94 p.p.m. The change from the value in CD_3CN presumably reflects the greater extent of

---

[*] These authors used an alternative sign convention which results in the chemical shifts having negative values.

Table 6. Variation with scan rate of peak potentials for the 2–/3– redox couple of $[NEt_4]_2[Fe_4S_4(SC_6H_4NH_2\text{-}4)_4]$ examined by cyclic voltammetry

Scan rate/mV s^{-1}	E_{pc}/V	E_{pa}/V	ΔP/mV	$i_{pc}v^{-\frac{1}{2}}$/μA dm^3 mmol^{-1} mV$^{-\frac{1}{2}}$ s$^{\frac{1}{2}}$
20	−1.19	−1.12	70	1.23
50	−1.20	−1.12	80	1.27
100	−1.21	−1.11	100	1.20
200	−1.22	−1.11	110	1.13

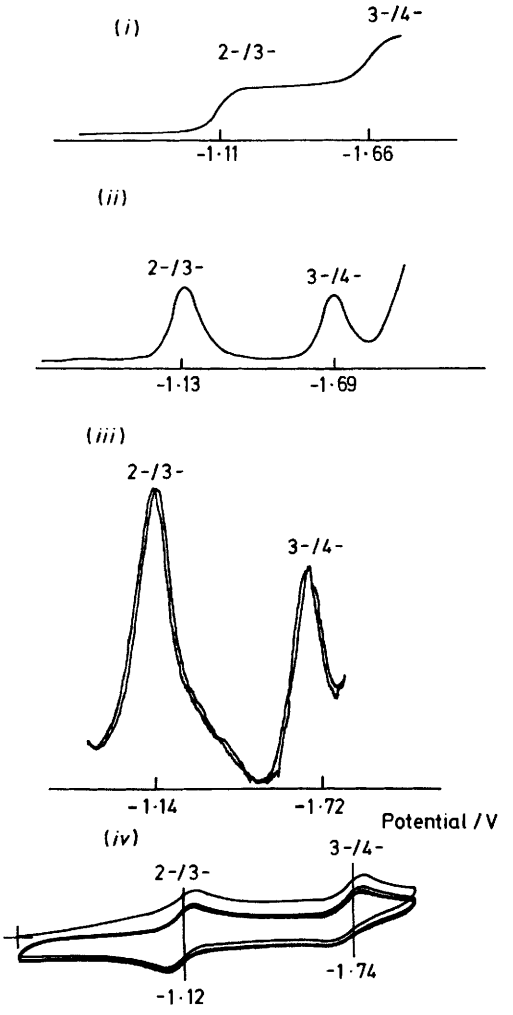

Figure 4. Polarographic and cyclic voltammetric characteristics of $[NEt_4]_2[Fe_4S_4(SC_6H_4NH_2\text{-}4)_4]$ in dmf solution: (*i*) d.c. polarogram; (*ii*) differential pulse polarogram; (*iii*) a.c. polarogram; and (*iv*) cyclic voltammogram

hydrogen bonding which occurs in $(CD_3)_2SO$. Isotropic shifts of the thiolate protons at 25 °C are compared with those of related clusters in Table 4. The temperature dependences of the isotropic shifts of $[Fe_4S_4(SC_6H_4NH_2\text{-}4)_4]^{2-}$ are shown in Figure 3. The broad-band ^{1}H-decoupled ^{13}C n.m.r. spectrum (75.4 MHz) of the compound was recorded in $(CD_3)_2SO$ solution and assigned *via* selective decoupling of protons. Chemical shift values (p.p.m.) of 196.1 (C bonded to S), 162.4 (*ortho*-C), 110.1 (*meta*-C), and 154.0 (*para*-C, bonded to NH_2) were observed.

Redox Properties.—The electron-transfer behaviour of $[NEt_4]_2[Fe_4S_4(SC_6H_4NH_2\text{-}4)_4]$ was investigated by Polarographic and cyclic voltammetric techniques in dmf solution. The recorded data are collected in Table 5 and current–voltage curves are shown in Figure 4. Two redox processes were observed at −1.12 and −1.74 V *vs.* s.c.e. which have been assigned, on the basis of previous studies,[17] to the 2–/3– and 3–/4– redox couples of the $[Fe_4S_4(SR)_4]^{2-}$ centre.

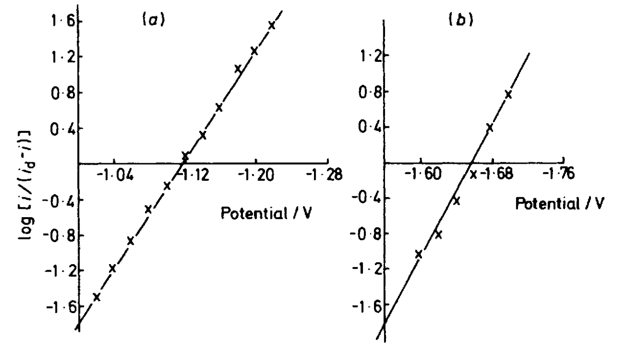

Figure 5. Plots of log $[i/(i_d - i)]$ *vs.* potential in V for the 2–/3– (*a*) and 3–/4– (*b*) reductions of $[NEt_4]_2[Fe_4S_4(SC_6H_4NH_2\text{-}4)_4]$

From the d.c. polarogram, voltage ranges corresponding to 25—75% of i_d were obtained as 65 and 50 mV for the 2–/3– and 3 – /4 – redox couples, respectively. Plots of log$[i/(i_d - i)]$ *vs.* potential in V (Figure 5) are linear and have slopes of −71 and −53 mV for the 2–/3– and 3–/4– redox couples, respectively. The respective differential pulse polarogram peak half-widths for these couples are 115 and 105 mV. These results are consistent with quasi-reversible, one-electron transfer for both redox processes.

The 2–/3– redox process was further examined by cyclic voltammetry and the observed variation of the peak separation, ΔP, with scan rate is detailed in Table 6. The current function $i_{pc}/v^{\frac{1}{2}}$ is essentially independent of scan rate over the range $20 < v < 200$ mV s^{-1}, satisfying the criteria for reversible electron transfer.[18] However, ΔP only approaches the theoretical value of 57 mV for an $n = 1$ process at slower scan rates, and increases as v increases. This behaviour is consistent with a quasi-reversible electrode process. For the 3–/4– redox couple $i_{pc} \gg i_{pa}$, indicating rapid decomposition of the reduced $[Fe_4S_4(SC_6H_4NH_2\text{-}4)_4]^{4-}$ species *via* chemical reaction.

During the cyclic voltammetric studies, small discontinuities were frequently observed at potentials between $E_{pc} = -0.90$ and −1.10 V, and $E_{pa} = -0.70$ and −0.80 V. These peaks were assigned to redox processes involving the 4-aminothiophenolate clusters bound to the microelectrode surface. No such peaks were observed during similar studies of $[NBu^n{}_4]_2[Fe_4S_4(SC_6H_5)_4]$.

The redox potentials of $[NEt_4]_2[Fe_4S_4(SC_6H_4NH_2\text{-}4)_4]$ in dmf solution are very similar to those of $[NMe_4]_2[Fe_4S_4(SC_6H_4NMe_2\text{-}4)_4]$, which (in dmf solution *vs.* s.c.e.) occur at −1.14 and −1.795 V for the 2–/3– and 3–/4– redox couples, respectively.[17] These potentials are in general more negative that the equivalent potentials of $[NEt_4]_2[Fe_4S_4(SPh)_4]$, which occur at −1.04 and −1.75 V under the same conditions.[17] This difference is ascribed to the electron-releasing effect of a 4-NR_2 substituent, which makes reduction of the cluster more difficult.

Acknowledgements

We thank the S.E.R.C. for the award of a studentship (to T. J. O.), the Fonds der Chemischen Industrie for financial support (to W. C. during crystallographic work undertaken at the University of Göttingen), and Mr. S. Bristow for recording the ^{13}C n.m.r. spectrum.

References

1 R. H. Holm, *Acc. Chem. Res.*, 1977, **10**, 427.

2 R. H. Holm and J. A. Ibers, in 'Iron-Sulfur Proteins,' ed. W. Lovenberg, Academic Press, New York, 1977, vol. 3, ch. 7.

3 J. M. Berg and R. H. Holm, in 'Metal Ions in Biology,' ed. T. G. Spiro, Wiley-Interscience, New York, 1982, vol. 4, ch. 1.

4 P. K. Mascharak, K. S. Hagen, J. T. Spence, and R. H. Holm, *Inorg. Chim. Acta*, 1983, **80**, 157.

5 L. Que, jun., M. A. Bobrik, J. A. Ibers, and R. H. Holm, *J. Am. Chem. Soc.*, 1974, **96**, 4168.

6 G. Christou, C. D. Garner, M. G. B. Drew, and R. Cammack, *J. Chem. Soc., Dalton Trans.*, 1981, 1550.

7 H. L. Carrell, J. P. Glusker, R. Job, and T. C. Bruice, *J. Am. Chem. Soc.*, 1977, **99**, 3683.

8 R. E. Johnson, G. C. Papaefthymiou, R. B. Frankel, and R. H. Holm, *J. Am. Chem. Soc.*, 1983, **105**, 7280.

9 E. T. Adman, L. C. Sieker, and L. H. Jensen, *J. Biol. Chem.*, 1976, **251**, 3801 and refs. therein.

10 C. W. Carter, jun., *J. Biol. Chem.*, 1977, **252**, 7802 and refs. therein.

11 G. Christou and C. D. Garner, *J. Chem. Soc., Dalton Trans.*, 1979, 1093.

12 M. A. Bobrik, L. Que, jun., and R. H. Holm, *J. Am. Chem. Soc.*, 1974, **96**, 285.

13 W. Clegg, *Acta Crystallogr., Sect. A*, 1981, **37**, 22.

14 D. Rogers, *Acta Crystallogr., Sect. A*, 1981, **37**, 734.

15 'International Tables for *X*-Ray Crystallography,' Kynoch Press, Birmingham, 1974, vol. 4, pp. 99, 149.

16 G. M. Sheldrick, SHELXTL: An integrated system for solving, refining and displaying crystal structures from diffraction data, Göttingen, 1978.

17 B. V. DePamphillis, B. A. Averill, T. Herskovitz, L. Que, jun., and R. H. Holm, *J. Am. Chem. Soc.*, 1974, **96**, 4159.

18 R. S. Nicholson and I. Shain, *Anal. Chem.*, 1964, **36**, 706.

Received 2nd *January* 1985; *Paper* 5/002